The Capacity of Downlink Fading Channels with Variable Rate and Power

Andrea J. Goldsmith, *Member, IEEE*

***Abstract*—We obtain the Shannon capacity region of the downlink (broadcast) channel in fading and additive white Gaussian noise (AWGN) for time-division, frequency-division, and code-division. For all of these techniques, the maximum capacity is achieved when the transmitter varies the data rate sent to each user as their channels vary. This optimal scheme requires channel estimates at the transmitter; dynamic allocation of timeslots, bandwidth, or codes; and variable-rate and power transmission. For both AWGN and fading channels, nonorthogonal code-division with successive decoding has the largest capacity region, while time-division, frequency-division, and orthogonal code-division have the same smaller region. However, when all users have the same average received power, the capacity region for all these techniques is the same. In addition, the optimal nonorthogonal code is a multiresolution code which does not increase the signal bandwidth. Spread-spectrum code-division with successive interference cancellation has a similar rate region as this optimal technique, however, the region is reduced due to bandwidth expansion. We also examine the capacity region of nonorthogonal code-division without interference cancellation and of orthogonal code-division when multipath corrupts the code orthogonality. Our results can be used to bound the spectral efficiency of the downlink channel using time-division, frequency-division, and code-division, both with and without multiuser detection.**

***Index Terms*—Capacity region, code-division, downlink, fading, variable power, variable rate.**

I. Introduction

WIRELESS communication systems require efficient use of the limited available spectrum and the underlying fading channel. Methods to divide the spectrum among many users include frequency-division, time-division, code-division, and hybrid combinations of these methods. Although there have been many performance comparisons of these techniques for cellular systems [1]–[4], the Shannon capacity of a multicell system using any of these methods remains an open problem [5]. The difficulty in determining the capacity of a multicell system is incorporating frequency reuse and the corresponding interference models into Shannon's mathematical definitions of entropy and mutual information [6]. Some progress in evaluating the uplink channel capacity in multicell systems for simple time-invariant interference models was made in [7]. No analogous work has been done for the downlink channel. The downlink channel in this context refers to the link from a central transmitter to multiple receivers, for example, from a base station to mobile units in a cellular system. This channel is also called the broadcast channel in information theory literature.

A common approach to determining the capacity of a cellular system is to assume a given power control and spectrum-sharing policy, compute the received signal-to-noise ratio (SNR) distribution for each user under this policy, and use this distribution to determine the achievable rate for each user. This calculation was done analytically in [1] and [3], and via simulation in [4] and [8]. However, since this calculation makes *a priori* assumptions about the resource allocation strategy, it can only lower-bound the multicell capacity, which is a fundamental channel characteristic independent of the system design.

Since the multicell capacity calculation appears intractable, we consider the capacity region of the downlink corresponding to a single isolated cell. Thus there is one transmitter sending independent data to many different users, and the capacity region defines the maximum rates at which these users can simultaneously receive their data reliably. This yields an upper bound on the capacity of a single cell within a multicell system, when intercell interference is present. Our model is also applicable to the downlink of satellites, wireless local-area networks (LAN's), and indoor cellular systems where there is high isolation between cells.

The definition of channel capacity in the context of a wireless system depends on whether the model is a single-user channel, a multiuser channel, or a cellular system with frequency reuse. For single-user channels, we use the classical capacity definition, the Shannon capacity, which was shown in [6] to equal the maximum possible data rate for a given channel with arbitrarily small error probability. Note that Shannon capacity places no constraints on the complexity or delay of the system. The input signal alphabet is also unconstrained, except for an average transmit power constraint. Thus the Shannon capacity yields an optimistic bound on achievable performance. It can therefore be used to upper-bound the maximum spectral efficiency (bps/Hz) which can be achieved over a given channel [9]–[11], as a figure of merit for diversity techniques under different fading conditions [12], and as a performance criterion for system design [13], [14]. For downlink channels we define capacity as the Shannon capacity region [15]. This region defines the set of rate vectors which all users can maintain simultaneously on the same channel with arbitrarily small error probability. The Shannon capacity region of the downlink imposes an average power constraint on the transmitter, but

Manuscript received December 10, 1995; revised June 4, 1996. This work was supported in part by Pacific Bell and in part by NSF under Career Development Award NCR-9501452.

The author is with the Department of Electrical Engineering, California Institute of Technology, Pasadena, CA 91125 USA.

Publisher Item Identifier S 0018-9545(97)04635-5.

complexity and delay are unconstrained. Different methods of spectrum-sharing yield different capacity regions, as will be discussed in more detail below. The Shannon capacity region has been used to bound the maximum transmission rate for each user in code-division multiple access (CDMA) systems [16], [17] and to analyze spreading code design [18]–[20]. The maximum transmission rate for time-division and frequency-division is also bounded by their respective Shannon capacity regions. The advantage to studying the Shannon capacity for both single-user and multiuser channels is that it is a function of the channel alone, independent of implementation details or technology limitations.

The capacity definition for cellular channels with frequency reuse typically incorporates the reuse distance and out-of-cell interference [1], [21], [22], and the associated units are bps/Hz/area. Since we consider only a single cell, this definition is not appropriate in our analysis.

We first describe results for the Shannon capacity of a single-user fading channel when the channel fading is tracked by both the transmitter and receiver. This single-user channel capacity as a function of the fading distribution is given by (2) in Section II-B. The capacity is achieved when the transmitter adapts its transmit power, data rate, and coding scheme as the channel varies. In particular, the optimal power and rate adaptation is a "water-filling" in time, similar to the water-filling used to achieve capacity on frequency-selective fading channels [23], [24]. We also show numerical results for the single-user capacity of Rayleigh and lognormal fading channels, and compare them to the capacity achieved using a suboptimal power adaptation which inverts the channel fading. Although channel inversion is simpler to implement, since it effectively removes the signal fading, it also suffers a severe capacity penalty relative to the adaptive rate and power policy.

We then describe the Shannon capacity region for downlink channels with AWGN. In particular, we first review the Shannon capacity regions derived in [15] for time-division, frequency-division, and code-division. These capacity regions are given by (12), (15), and (17), respectively. Although in general each of these capacity regions are different, they reduce to the same region when all users have the same transmit power and noise statistics [25]. The maximum capacity region is obtained using multiresolution code-division with successive decoding. This technique is similar to spread-spectrum code-division with successive interference cancellation, except that no bandwidth expansion is required. We then obtain the capacity region of spread-spectrum code-division both with (19) and without (20) successive decoding. Without successive decoding, spread-spectrum code-division has the smallest capacity region of all the spectrum-sharing techniques. We also show that the capacity region with orthogonal spread-spectrum coding (18) is a subset of the time-division and frequency-division rate regions.

We combine the results of Section II for the single-user fading channel with those of Section III for the downlink channel with AWGN to obtain the capacity region of the downlink fading channel under the different spectrum-sharing techniques. These capacity regions for time-division, frequency-division, and code-division are given by (23), (26), and (27), respectively, which are functions of the fading distribution. We show that (27), corresponding to a variable-rate variable-power multiresolution code with adaptive decoding, has the maximum rate region for this channel. This technique is similar to variable-rate variable-power spread spectrum with adaptive interference cancellation. For time-division and frequency-division, adaptive power and bandwidth or timeslot allocation achieves the maximum rate region. As for the AWGN channel, the capacity region of the different spectrum-sharing techniques is the same if all users have the same transmit power and fading distribution. We obtain numerical results for the capacity regions in Rayleigh fading, and compare them with the AWGN capacity region. We will see that these capacity regions have the same relative shape, although the capacity regions in fading are smaller.

Our capacity results indicate that code-division with successive decoding or interference cancellation maximizes spectral efficiency. It should be emphasized that the optimality of this multiuser detection method, for both the AWGN and the fading channel, is only valid for Shannon capacity bounds, where the probability of decoding error is asymptotically small. The optimal multiuser detector in practice was derived by Verdú in [26]. Unfortunately, this optimal detector, which cancels interference between users in parallel, has complexity that increases exponentially with the number of users. A desire for less complex algorithms has led to research in many classes of suboptimal detectors, with the usual tradeoff between performance and complexity. Successive interference cancellation is a relatively simple technique, and has been shown to improve performance of CDMA systems relative to single-user detection [16], [27], [28]. However, the performance of successive interference cancellation is seriously degraded when incorrect decisions are made, since these decisions are used by subsequent iterations of the cancellation algorithm. This problem is exacerbated when the received signal power for each user is the same. Other multiuser detection schemes with improved performance relative to successive interference cancellation include the decorrelating detector [29], the minimum mean-square error (MMSE) detector [30], [31], decision-feedback detector [32], and multistage detector [33], [34]. A good tutorial survey of these different multiuser detection schemes, for both synchronous and asynchronous channels, can be found in [35]. This reference also discusses recent advances in multiuser detection for fading channels.

Our Shannon capacity results place no restriction on the transmitted signal alphabet, except for its average power. It has been shown recently that the capacity of memoryless channels with unconstrained inputs can be approximated with arbitrary precision using a finite set of inputs [37]. Moreover, it is known that restricting the signal envelope does not decrease capacity [38]. Binary inputs do reduce capacity, and a tight bound on this reduction can be found in [39]. The extension of these capacity results for single-user channels with restricted inputs to multiuser systems is beyond the scope of this paper. We believe, however, that restricting the input alphabets will not significantly change our capacity results, in that all the techniques we analyze will be equally affected by the restriction.

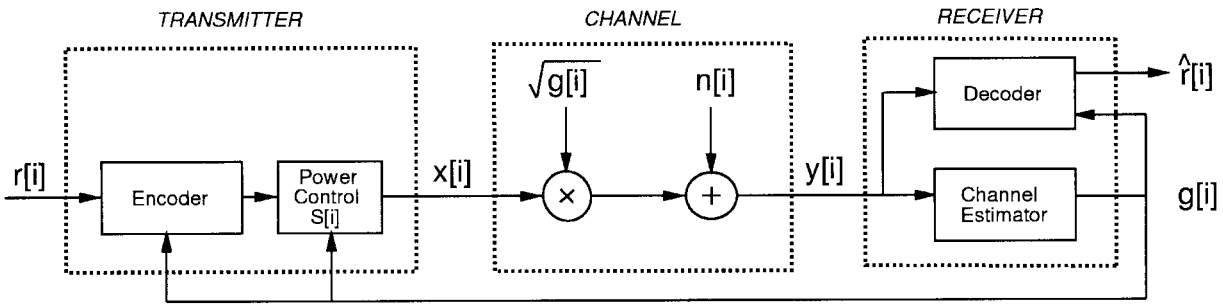

Fig. 1. System model.

The remainder of this paper is organized as follows. The capacity of the single-user fading channel with transmitter and receiver adaptation to the channel variation is presented in Section II. The capacity region of the downlink AWGN channel under the different spectrum-sharing techniques is analyzed in Section III. In Section IV we unify the previous results to obtain the capacity region of the downlink fading channel with channel adaptation. Our conclusions are summarized in the final section.

II. Single-User Fading Channels

A. System Model

Consider a discrete-time channel with stationary time-varying gain $\sqrt{g[i]}$ and AWGN $n[i]$. Let S denote the average transmit signal power, $N_0/2$ denote the noise density of $n[i]$, B denote the received signal bandwidth, and $\overline{g}$ denote the average channel gain. In general, we will use the notation $\overline{x}$ to denote the average, or expected, value of x. With appropriate scaling of S we can assume that $\overline{g} = 1$. The instantaneous received SNR is then $\gamma[i] = Sg[i]/(N_0B)$, and its average value is $\overline{\gamma} = S/(N_0B)$. We denote the distribution of γ by $p(\gamma)$, which we assume to be either lognormal (lognormal shadowing) or exponential (Rayleigh fading) in the numerical calculations below.

The system model is illustrated in Fig. 1. In this model, the channel power gain $g[i]$ is available to both the transmitter and receiver at time i. This allows the transmitter to adapt to the channel gain, and is a reasonable model for a slowly varying channel with channel estimation and transmitter feedback.

B. Channel Capacity

The capacity of a fading channel is limited by the available transmit power and bandwidth. Let $S(\gamma)$ denote the transmit power adaptation policy relative to an instantaneous received SNR of γ, subject to the average power constraint

$$\int_0^\infty S(\gamma)p(\gamma)\,d\gamma \le S. \tag{1}$$

The capacity of the fading channel with bandwidth B and $\overline{\gamma} = S$ under the assumptions outlined in Section II-A is derived in [40] to be

$$C[S, B] = \max_{S(\gamma):\ \int S(\gamma)p(\gamma)\,d\gamma = S} \int_0^\infty B \log\left[1 + \frac{S(\gamma)\gamma}{S}\right] \cdot p(\gamma)\,d\gamma. \tag{2}$$

Capacity in bits per second is obtained using the base 2 logarithm.

The power adaptation which maximizes (2) is

$$\frac{S(\gamma)}{S} = \begin{cases} \dfrac{1}{\gamma_0} - \dfrac{1}{\gamma}, & \gamma \ge \gamma_0 \\ 0, & \gamma < \gamma_0 \end{cases} \tag{3}$$

for some "cutoff" value γ_0. If the received signal power is below this level, then no power is allocated to data transmission. Since γ is time-varying, the maximizing transmit power distribution (3) is a "water-filling" formula in time that depends on the fading statistics only through the cutoff value γ_0. This water-filling is illustrated in Fig. 2.

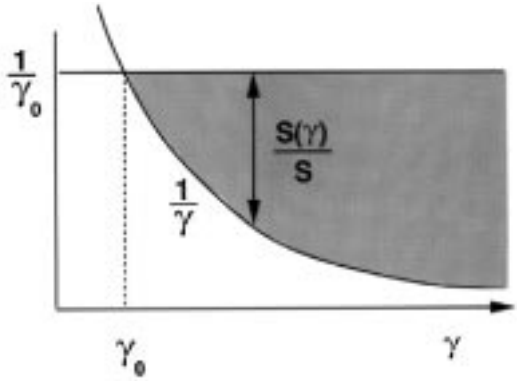

Fig. 2. Water-filling power adaptation.

Substituting (3) into (1), we see that γ_0 is determined by numerically solving

$$\int_{\gamma_0}^\infty \left(\frac{1}{\gamma_0} - \frac{1}{\gamma}\right)p(\gamma)\,d\gamma = 1. \tag{4}$$

Once γ_0 is known, we substitute (3) into (2) to get

$$C[S, B] = B\int_{\gamma_0}^\infty \log\left(\frac{\gamma}{\gamma_0}\right)p(\gamma)\,d\gamma. \tag{5}$$

The channel coding and decoding strategy which achieves this capacity is a multiplexing technique, as shown in Fig. 3.

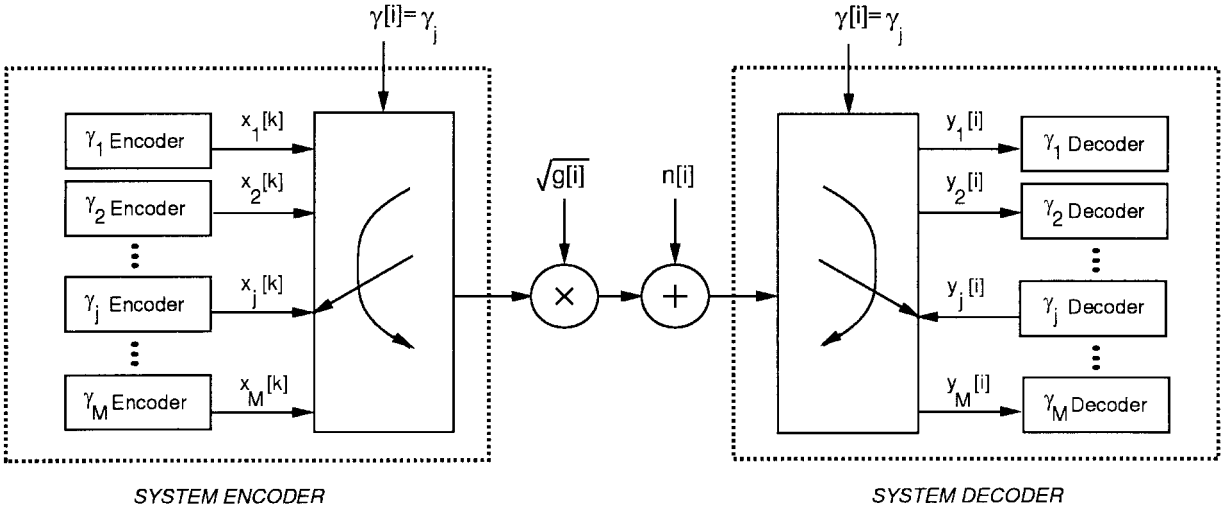

Fig. 3. Multiplexed coding and decoding.

Specifically, for each possible fade level γ_j, the optimal Shannon code relative to an AWGN channel with attenuation γ_j is designed according to the random coding process described in [6]. This code is transmitted over the channel whenever the fade level $\gamma[i] = \gamma_j$. This multiplexed transmission scheme is both variable-power and variable-rate, since the code rates designed for different γ_j fade levels will be different. In [40], we show that this multiplexing strategy achieves the channel capacity (5) and that no other transmission method can achieve a higher capacity. In practice, the multiplexing concept can be implemented with variable-rate and power MQAM. This technique is shown in [41] to achieve rates within 8 dB of the capacity limit, and this gap can be further reduced with coding [42].

Note that for a constant transmit power $S(\gamma) = S$, the capacity of (2) reduces to

$$C[S, B] = B \log \int_0^\infty (1+\gamma) p(\gamma)\, d\gamma \tag{6}$$

which was previously reported by Lee as the average channel capacity [12]. In fact, (6) is the Shannon capacity of the channel when the transmitter uses the multiplexing code strategy of Fig. 3, with each of the γ_j codes restricted to the same constant transmit power. Surprisingly, the difference between (2) and (6) is negligible in both Rayleigh fading and lognormal shadowing [40]. Thus while rate adjustment relative to the channel variation is critical for efficient transmission, power adaptation is not. Moreover, if the channel fading is independent from symbol to symbol then (6) can also be achieved using a nonadaptive coding strategy. More details on this nonadaptive strategy can be found in [40].

C. Channel Inversion

In this section, we consider a suboptimal power adaptation policy where the transmitter adjusts its power to maintain a constant received power, i.e., the transmitter inverts the channel fading. The channel then appears to the encoder and decoder as a time-invariant AWGN channel, and thus the complexity of its code design is much simpler than with the adaptive policy. The power control policy for channel inversion is $S(\gamma)/S = \sigma/\gamma$, where σ equals the received SNR that can be maintained subject to the average power constraint. Thus the constant σ satisfies $\int (\sigma/\gamma) p(\gamma) = 1$, so $\sigma = 1/\overline{[1/\gamma]}$.

The channel capacity with this power adaptation strategy is derived from the capacity of an AWGN channel with average power σ [6]

$$C[S, B] = B \log[1+\sigma] = B \log\left[1 + \frac{1}{\overline{[1/\gamma]}}\right]. \tag{7}$$

This form of power adaptation greatly simplifies the coding strategy for the fading channel, since the channel with inversion appears to the encoder and decoder as an AWGN channel, independent of the fading statistics.

The inversion form of power adaptation requires that much of the transmit power be used to compensate for deep fading. We therefore also consider a truncated inversion policy that only compensates for fading above a certain cutoff fade depth γ_0

$$\frac{S(\gamma)}{S} = \begin{cases} \dfrac{\sigma}{\gamma}, & \gamma \geq \gamma_0 \\ 0, & \gamma < \gamma_0. \end{cases} \tag{8}$$

Since the channel is only used when $\gamma \geq \gamma_0$, the power constraint (1) yields $\sigma = 1/\overline{[1/\gamma]}_{\gamma_0}$, where

$$\overline{[1/\gamma]}_{\gamma_0} \triangleq \int_{\gamma_0}^\infty \frac{1}{\gamma} p(\gamma)\, d\gamma. \tag{9}$$

The capacity is thus

$$C[S, B] = B\left[1 + \frac{1}{\overline{[1/\gamma]}_{\gamma_0}}\right] p(\gamma \geq \gamma_0) \tag{10}$$

where

$$p(\gamma \geq \gamma_0) = \int_{\gamma_0}^\infty p(\gamma)\, d\gamma.$$

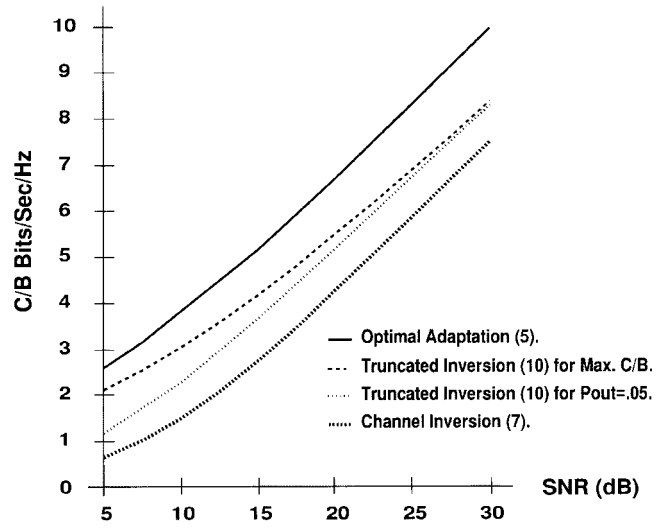

Fig. 4. Capacity in lognormal fading.

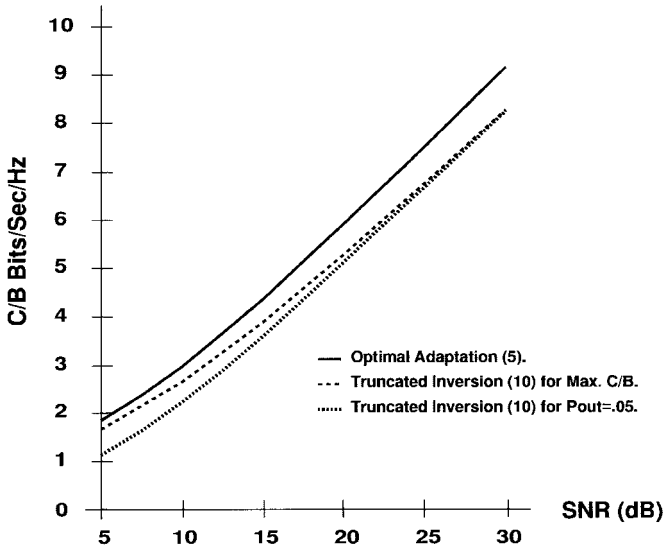

Fig. 5. Capacity in Rayleigh fading.

To get the maximum capacity for this truncated channel inversion policy, we maximize (10) relative to γ_0. Alternatively, we can set γ_0 to achieve a desired outage probability $P_{\text{out}} = p(\gamma < \gamma_0)$. We will see in the next section that without truncation, the channel inversion policy yields a capacity of zero for Rayleigh fading channels.

D. Numerical Results

Fig. 4 shows a plot of (5), (7), and (10) (for different γ_0 criteria) as a function of SNR for lognormal fading with a standard deviation of 8 dB. Note that for this range of SNR, the capacity (5) in shadowing exceeds that of the AWGN channel: $C = B\log(1+\text{SNR})$. For Rayleigh fading, $\overline{[1/\gamma]}$ is infinite: thus the spectral efficiency with the channel inversion policy is zero. Fig. 5 shows the capacity of the other policies in Rayleigh fading, which is less than the capacity in AWGN. We also see from these figures that truncated channel inversion exhibits a 1- to 5-dB rate penalty, and channel inversion without truncation can yield a very large capacity loss. In addition, maintaining a fixed outage probability at low SNR's causes some loss relative to the maximum C/B obtained with truncated inversion, but this loss diminishes with increasing SNR. Although these conclusions apply to the Shannon capacity, which is an asymptotic result without complexity or delay constraints, we have found analogous results for practical transmission schemes. Specifically, in [41] it is shown that the spectral efficiency of variable-rate variable-power MQAM exhibits a 5–10-dB gain over fixed-rate MQAM with truncated channel inversion.

III. The AWGN Downlink Channel Capacity Region

When several users share the same channel, the channel capacity can no longer be characterized by a single number. At the extreme, if only one user occupies the channel then the single-user capacity results of the previous section apply. However, since there is an infinite number of ways to "divide" the channel between many users, the multiuser channel capacity is characterized by a *rate region*, where each point in the region is a vector of achievable rates that can be maintained by all the users simultaneously. The closure of the union of all achievable rate vectors is called the *capacity region* of the multiuser system.

In this section, we analyze the capacity region of a downlink channel with AWGN. We begin by first reviewing results from [15, Sec., 14.6] for the AWGN downlink channel capacity region using superposition code-division with successive decoding, time-division, and frequency-division. We then extend the code-division analysis to direct sequence spread spectrum for both orthogonal and nonorthogonal codes, and obtain the corresponding capacity regions both with and without successive decoding.

We will see that the maximum-capacity region is achieved using a multiresolution code with successive decoding. In addition, spread-spectrum code-division with successive decoding has a capacity penalty relative to this optimal code which increases with spreading gain. Finally, spread spectrum with orthogonal code-division can achieve a subset of the time-division and frequency-division capacity regions, but spread spectrum with nonorthogonal coding and no successive decoding is inferior to all the other spectrum-sharing techniques.

A. The AWGN Downlink Channel Model

The downlink channel consists of one transmitter sending *independent* information to different receivers over a common channel. Thus it does not model a typical FM radio or TV broadcast channel, where the same signal is received by all users. The capacity region of the broadcast channel characterizes the rates at which information can be conveyed to the different receivers simultaneously. We only consider capacity regions for the two-user downlink channel, since it is the easiest to illustrate. The general properties and the relative performance of the different spectrum-sharing techniques for a larger number of users are the same as in the two-dimensional case [25]: since the distribution of the transmitted signal which achieves the multiuser capacity region is Gaussian for each

user [15], interference from other users is accurately modeled as Gaussian noise even for a small number of interferers.

We will use the following notation. The two-user downlink channel has one transmitter and two distant receivers receiving data at rate R_i, $i = 1, 2$. Each receiver has front-end AWGN of noise density n_i, $i = 1, 2$, and we arbitrarily assume $n_1 \leq n_2$. We denote the transmitter's total average power and bandwidth by S and B, respectively.

If the transmitter allocates all the power and bandwidth to one of the users, then clearly the other user will have a rate of zero. Therefore, the set of simultaneously achievable rates (R_1, R_2) includes the pairs $(C_1, 0)$ and $(0, C_2)$, where

$$C_i = B \log \left[1 + \frac{S}{n_i B}\right]. \tag{11}$$

These two points bound the downlink capacity region. We now consider rate pairs in the interior of the region, which are achieved using more equitable methods of dividing the system resources.

B. Time-Division

In time-division, the transmit power S and bandwidth B are allocated to user 1 for a fraction τ of the total transmission time, and then to user 2 for the remainder of the transmission. This time-division scheme achieves a straight line between the points C_1 and C_2, corresponding to the rate pairs

$$\left\{\bigcup [R_1 = \tau C_1,\, R_2 = (1-\tau)C_2]; \quad 0 \leq \tau \leq 1\right\}. \tag{12}$$

This equal-power time-division capacity region is illustrated in Figs. 7 and 8. In these figures, $n_1 B$ and $n_2 B$ differ by 3 and 20 dB, respectively. This decibel difference is a crucial parameter in comparing the relative capacities of the different spectrum-sharing techniques, as we discuss in more detail below.

If we also vary the average transmit power of each user then we can achieve a larger capacity region. Let S_1 and S_2 denote the average power allocated to users 1 and 2 over their respective time slots. The average transmit power constraint then becomes $\tau S_1 + (1-\tau)S_2 = S$. The capacity region with this power allocation is then

$$\left\{\bigcup \left(R_1 = \tau B \log \left[1 + \frac{S_1}{n_1 B}\right], \right.\right.$$
$$\left. R_2 = (1-\tau) B \log \left[1 + \frac{S_2}{n_2 B}\right]\right);$$
$$\left.\tau S_1 + (1-\tau) S_2 = S,\, 0 \leq \tau \leq 1\right\}. \tag{13}$$

We will see in the following section that the rate region defined by (13) is the same as the frequency-division capacity region.

C. Frequency-Division

In frequency-division, the transmitter allocates S_i of its total power S and B_i of its total bandwidth B to user i. The power and bandwidth constraints require that $S_1 + S_2 = S$ and $B_1 + B_2 = B$. The set of achievable rates for a fixed frequency division (B_1, B_2) is thus

$$\left\{\bigcup \left(R_1 = B_1 \log \left[1 + \frac{S_1}{n_1 B_1}\right], \right.\right.$$
$$\left. R_2 = B_2 \log \left[1 + \frac{S_2}{n_2 B_2}\right]\right);\; S_1 + S_2 = S\right\}. \tag{14}$$

It was shown by Bergmans [25] that, for n_1 strictly less than n_2 and any fixed frequency-division (B_1, B_2), there exists a range of power allocations $\{S_1, S_2\colon S_1 + S_2 = S\}$ whose corresponding rate pairs exceed a segment of the equal-power time-division line (12).

The frequency-division rate region is defined as the union of fixed frequency-division rate regions (14) over all bandwidth divisions

$$\left\{\bigcup \left(R_1 = B_1 \log \left[1 + \frac{S_1}{n_1 B_1}\right], \right.\right.$$
$$R_2 = B_2 \log \left[1 + \frac{S_2}{n_2 B_2}\right]\Big);$$
$$\left. S_1 + S_2 = S,\, B_1 + B_2 = B\right\}. \tag{15}$$

It was shown in [25] that this capacity region exceeds the equal-power time-division rate region (12). This superiority is indicated by interpolating between the fixed frequency-division regions in Figs. 7 and 8, although it is difficult to see in Fig. 7, where the users have a similar received SNR. In fact, when $n_1 = n_2$, the frequency-division capacity region (15) reduces to the time-division region (12) [25]. Thus optimal power and/or frequency allocation is more beneficial when the users have very disparate channel quality.

Note that the rate region for time-division with unequal power allocation given by (13) is the same as the frequency-division rate region (15). This is seen by letting $B_i = \tau_i B$ and $\sigma_i = \tau_i S_i$ in (13), where $\tau_1 = \tau$ and $\tau_2 = 1 - \tau$. The power constraint then becomes $\sigma_1 + \sigma_2 = S$. Making these substitutions in (13) yields

$$\left\{\bigcup \left(R_1 = B_1 \log \left[1 + \frac{\sigma_1}{n_1 B_1}\right], \right.\right.$$
$$\left. R_2 = B_2 \log \left[1 + \frac{\sigma_2}{n_2 B_2}\right]\right);\; \sigma_1 + \sigma_2 = S\right\}. \tag{16}$$

Comparing this with (14) we see that with appropriate choice of S_i and τ_i, any point in the frequency-division rate region can also be achieved through time-division with unequal power allocation.

D. Code-Division (CD)

Superposition coding with successive decoding, described in more detail in [15], is a multiresolution coding technique whereby the user with the more favorable channel can distinguish the fine resolution of the received signal constellation, while the user with the worse channel can only distinguish the constellation's coarse resolution. An example of a two-level multiresolution code constellation taken from [43] is 32-QAM with embedded 4-PSK, as shown in Fig. 6. In this

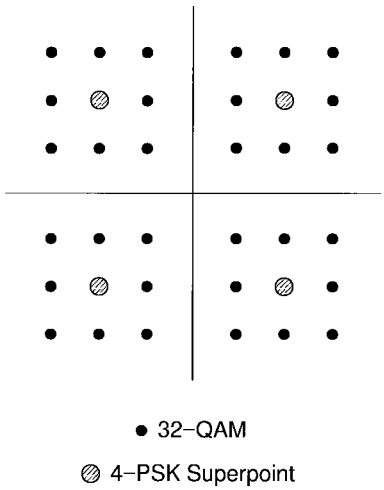

Fig. 6. 32-QAM with embedded 4-PSK.

example, the user with the better SNR, User 1, transmits three bits per symbol time. User 2, with a worse SNR than User 1, transmits two bits per symbol time. The transmitted constellation point is one of the 32-QAM signal points chosen as follows. User 2 provides two bits to select one of the 4-PSK superpoints. User 1 provides three bits to select one of the eight constellation points surrounding the selected superpoint. After transmission through the channel, User 1 can easily distinguish the quadrant in which the constellation point lies. Thus the 4-PSK superpoint of User 2 is subtracted out in User 1's demodulation. However, User 2 cannot distinguish between the 32-QAM points around its 4-PSK superpoints. Thus the 32-QAM modulation superimposed on the 4-PSK modulation appears as noise to User 2. These ideas can be easily extended to multiple users with multiple transmission rates using more complex signal constellations. Since superposition coding achieves multiple rates by expanding its signal constellation, it does not typically require bandwidth expansion. The successive decoding process is also simpler than spread-spectrum multiuser detection methods.

The two-user capacity region using multiresolution coding and successive decoding was derived in [25] to be the set of rate pairs

$$\left\{\bigcup\left(R_1 = B\log\left[1+\frac{S_1}{n_1 B}\right], \quad R_2 = B\log\left[1+\frac{S_2}{n_2 B+S_1}\right]\right);\ S_1+S_2=S\right\}. \quad (17)$$

The intuitive explanation for (17) is the same as for the example discussed above. Since $n_1 < n_2$, User 1 correctly receives all the data transmitted to User 2. Therefore, User 1 can decode and subtract out User 2's message, then decode its own message. User 2 cannot decode the message intended for User 1, since it has a less-favorable channel; thus User 1's message, with power S_1, contributes an additional noise term to User 2's received message. This same process is used by the successive interference canceler in spread-spectrum systems [16].

The rate region defined by (17) was shown in [44] to exceed the regions achievable through either time- or frequency-division, when $n_1 < n_2$. Moreover, it was also shown in [44] that this is the maximum achievable set of rate pairs for any type of coding and spectrum sharing, and thus (17) defines the capacity region. However, if the users all have the same SNR, then this capacity region collapses to the equal-power time-division line (12). Thus when $n_1 = n_2$, all the spectrum-sharing methods have the same rate region.

Code-division can also be implemented using direct-sequence spread spectrum [45]. With spread-spectrum codes, the modulated data signal is multiplied by a spreading code, which increases the transmit signal bandwidth by a factor G, called the spreading gain. For orthogonal spreading codes, the crosscorrelation between the respective codes is zero. Orthogonal coding in the cellular IS-95 standard is implemented using Hadamard–Walsh functions [16]. These functions require a spreading gain of N to produce N orthogonal codes. For a total bandwidth constraint B, the information bandwidth of each user's signal with these spreading codes is thus limited to B/N. The two-user rate region with these spreading codes is then

$$\left\{\bigcup\left(R_1 = \frac{B}{2}\log\left[1+\frac{S_1}{\frac{n_1 B}{2}}\right], \quad R_2 = \frac{B}{2}\log\left[1+\frac{S_2}{\frac{n_2 B}{2}}\right]\right);\ S_1+S_2=S\right\}. \quad (18)$$

Comparing (18) with (14) we see that code-division with orthogonal coding is the same as fixed frequency-division with the bandwidth equally divided ($B_1 = B_2 = B/2$). From (16), time-division with unequal power allocation can also achieve all points in this capacity region. Thus orthogonal code-division with Hadamard–Walsh functions achieves a subset of the time-division and frequency-division capacity regions. More general orthogonal codes are needed to achieve the same region as these other techniques.

We now consider spread spectrum with nonorthogonal spreading codes. These codes are commonly generated using maximal length shift registers [46], which yield a code crosscorrelation of approximately $1/G$. Thus interference between users is attenuated by a factor of G. Since the signal bandwidth is also increased by this factor, the information bandwidth of the signal reduces to B/G. The two-user rate region using maximal-length spread-spectrum codes and successive decoding is thus given by

$$\left\{\bigcup\left(R_1 = \frac{B}{G}\log\left[1+\frac{S_1}{\frac{n_1 B}{G}}\right], \quad R_2 = \frac{B}{G}\log\left[1+\frac{S_2}{\frac{n_2 B}{G}+\frac{S_1}{G}}\right]\right);\ S_1+S_2=S\right\}. \quad (19)$$

Note that (17) and (19) differ only by the parameter $G \geq 1$. By the convexity of the log function, the rate region defined by (19) for $G > 1$ is smaller than the rate region (17) obtained

using superposition coding, and the degradation increases with increasing values of G. This implies that for nonorthogonal coding, the spreading gain should be minimized in order to maximize capacity.

With maximal-length spreading codes and no successive decoding, the receiver treats all signals intended for other users as noise, resulting in the rate region [16]

$$\left\{\bigcup\left(R_1=\frac{B}{G}\log\left[1+\frac{S_1}{\frac{n_1B}{G}+\frac{S_2}{G}}\right],\right.\right.$$
$$\left.\left.R_2=\frac{B}{G}\log\left[1+\frac{S_2}{\frac{n_2B}{G}+\frac{S_1}{G}}\right]\right);\ S_1+S_2=S\right\}. \quad (20)$$

Again using the log function convexity, $G=1$ maximizes this rate region, and the rate region decreases as G increases. For $G=1$, (20) corresponds to superposition coding without successive decoding, i.e., a coding technique whereby all the users' signals are superimposed on top of each other, and the decoding process treats all signals except the desired signal as noise.

The radius of curvature for (20) is given by

$$\chi=\frac{\dot{R}_1\ddot{R}_2-\dot{R}_2\ddot{R}_1}{(\dot{R}_1^2+\dot{R}_2^2)^{3/2}} \quad (21)$$

where $\dot{R}_i$ and $\ddot{R}_i$ denote, respectively, the first and second derivatives of R_i with respect to τ, for $S_1=\tau S$ and $S_2=(1-\tau)S$. For $G=1$, $\chi\geq 0$. Thus the rate region for nonorthogonal coding without successive decoding (20) is bounded by a convex function with endpoints C_1 and C_2, as shown in Figs. 7 and 8. Therefore, the capacity region for nonorthogonal code-division without successive decoding will lie beneath the regions for time-division and frequency-division, which are bounded by concave functions with the same endpoints. Interestingly, as $G\to\infty$, the sign of χ changes. Thus as the capacity region decreases with large G, it also becomes concave.

While the orthogonality of time-division and frequency-division is relatively robust against small multipath delays introduced by the channel, the orthogonality of the Hadamard–Walsh functions is destroyed by multipath delays bigger than a chip time [45]. This loss of orthogonality causes interference noise between users, so the rate region becomes

$$\left\{\bigcup\left(R_1=\frac{B}{G}\log\left[1+\frac{S_1}{\frac{n_1B}{G}+\frac{S_2}{G'}}\right],\right.\right.$$
$$\left.\left.R_2=\frac{B}{G}\log\left[1+\frac{S_2}{\frac{n_2B}{G}+\frac{S_1}{G'}}\right]\right);\ S_1+S_2=S\right\} \quad (22)$$

where $1/G'$ equals the code crosscorrelation with multipath. If $G'\approx G$ then the rate region defined by (22) is approximately the same as (20). As the multipath effect diminishes, $G'\to\infty$ and the region (22) converges to (18).

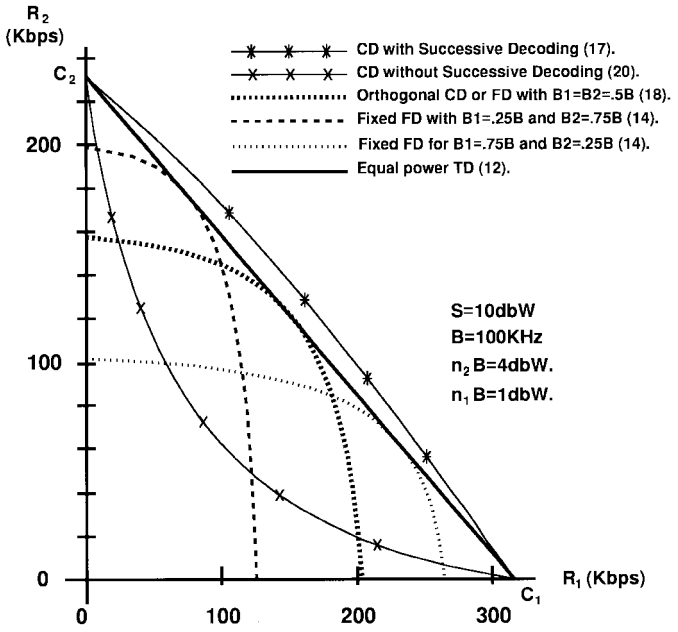

Fig. 7. Two-user capacity region: 3-dB SNR difference.

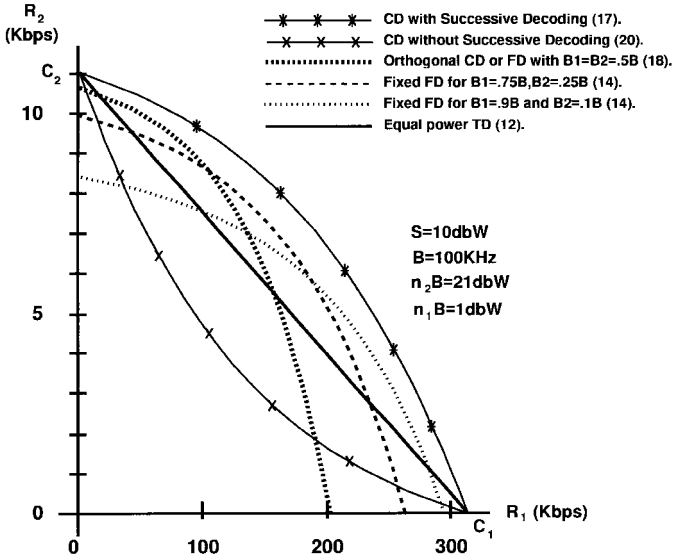

Fig. 8. Two-user capacity region: 20-dB SNR difference.

The rate regions for equal-power time-division (12), frequency-division (14), orthogonal code-division (18), and nonorthogonal code-division with (17) and without (20) successive decoding are illustrated in Figs. 7 and 8. The two figures correspond to an SNR difference between the users of 3 and 20 dB, respectively. Both code-division capacity regions assume $G=1$, i.e., the coding technique is superposition coding with or without successive decoding. If spread spectrum is used instead, the capacity regions will decrease as the spreading gain G increases. Note that the capacity regions for all the spectrum-sharing techniques nearly coincide when the user SNR's differ by just 3 dB, whereas a 20-dB difference results in a large capacity difference between the different methods.

IV. The Downlink Channel with Fading and AWGN

We now combine the capacity analysis in Section II for the single-user fading channel with the capacity region analysis in Section III to obtain the capacity region of the fading broadcast channel.

A. The Fading Downlink Channel Model

The two-user downlink channel with fading and AWGN has one transmitter with average power S and bandwidth B and two receivers with noise density N_j and time-varying received SNR $\gamma_j[i] = Sg_j[i]/(N_jB)$, $j = 1, 2$. Let $n_j[i] = N_j/g_j[i]$, so $\gamma_j[i] = S/(n_j[i]B)$. We assume that both $n_1[i]$ and $n_2[i]$ are known to the transmitter and both receivers at time i. Thus the transmitter can vary its power $S[i]$ relative to $n_1[i]$ and $n_2[i]$, subject only to the average power constraint S. For frequency-division, it can also vary the bandwidth $B_j[i]$ allocated to each user, subject to the constraint $B_1[i]+B_2[i] = B$ for all i. Finally, for code-division, the superposition code can be varied at each transmission. Since both receivers know the noise density pairs $n_1[i]$ and $n_2[i]$, they can decode their individual signals based on the known resource allocation strategy given these noise densities. In practice, the transmitter strategy would need to be conveyed to each receiver through either a pilot tone or a header on the transmitted data.

B. Time-Division

Since time-division allocates orthogonal time slots to each user, the two-user channel with time-division reduces to two orthogonal time-varying single-user channels. Thus we can apply the single-user capacity results in Section II-B to each of the two channels. This yields the rate region

$$\left\{\bigcup (R_1 = \tau C_1[S, B], R_2 = (1-\tau)C_2[S, B]);\ 0 \le \tau \le 1\right\} \tag{23}$$

where $C_i[S, B]$, $i = 1, 2$, is given by (5), (7), or (10), depending on the power adaptation strategy. Clearly, the maximum capacity region has $C_i[S, B]$ given by (5), corresponding to the maximum single-user capacity.

The strategy to achieve the maximum capacity of the time-division channel requires each user to adapt its power and rate optimally over his assigned timeslot. Specifically, User 1 transmits the code which achieves its fading channel capacity $C_i[S, B]$ over a fraction τ of the total transmission time, and User 2 transmits its optimal code over the remaining time. The optimal code designs are identical to the capacity-achieving code designs described in Section II-B.

If the average power allocated to each user is different, the capacity region becomes

$$\left\{\bigcup (R_1 = \tau C_1[S_1, B], R_2 = (1-\tau)C_2[S_2, B]);\ \tau S_1 + (1-\tau)S_2 = S,\ 0 \le \tau \le 1\right\}. \tag{24}$$

As for the AWGN channel, the unequal-power time-division rate region (24) is equivalent to the fixed frequency-division rate region (25) obtained below.

C. Frequency-Division

Fixed frequency-division divides the total channel bandwidth B into nonoverlapping segments of width B_1 and B_2, which also reduces the two-user channel to independent single-user channels. As in the time-division case, we can thus apply the optimal code design and corresponding capacity results of Section II-B to each channel independently, yielding the fixed frequency-division rate region

$$\left\{\bigcup (R_1 = C[S_1, B_1], R_2 = C[S_2, B_2]);\ S_1 + S_2 = S\right\}. \tag{25}$$

Again, $C[S_i, B_i]$ is given by (5), (7), or (10), with (5) achieving the maximum capacity region. Setting $B_1 = \tau B$ and $S_1 = \tau S$ in (25) and comparing with (24) shows the equivalence of unequal-power time-division and fixed frequency-division on the fading channel.

It is clear that the equal-power time-division capacity region (23) will exceed the fixed frequency-division rate region over some range of power allocations $\{S_1, S_2\colon S_1 + S_2 = S\}$, in particular when all of the power is allocated to one of the frequency bands. Suppose, however, that both the power and the bandwidth partition vary at each transmission based on the instantaneous noise densities $n_1[i]$ and $n_2[i]$. Clearly, the resulting rate region will exceed both fixed frequency-division and time-division, which fixes the allocation of these resources over all time. The rate region for this variable power and bandwidth allocation scheme is

$$\left\{\bigcup \left(R_1 = \int_k C_{1,k}[S_{1,k}, B_{1,k}]\pi_k,\ R_2 = \int_k C_{2,k}[S_{2,k}, B_{2,k}]\pi_k\right);\ B_{1,k} + B_{2,k} = B,\ \int_k (S_{1,k} + S_{2,k})\pi_k = S\right\} \tag{26}$$

where π_k denotes the joint noise density distribution

$$\pi_k = p(n_1[i] = n_{1,k},\ n_2[i] = n_{2,k})$$

$S_{j,k}$ and $B_{j,k}$ are the bandwidth and power allocated to user j when $n_j[i] = n_{j,k}$, and

$$C_{j,k}[S_{j,k}, B_{j,k}] = B_{j,k} \log [1 + S_{j,k}/(n_{j,k}B_{j,k})].$$

To determine the boundary region of (26), both the power and bandwidth allocations must be optimized jointly over time, so the two users are no longer independent. Finding this boundary region requires an exhaustive search or a multidimensional optimization over time subject to the bandwidth and power constraints. We do not evaluate this region in the numerical results presented below. However, this capacity region is bounded above by the capacity region for superposition coding with successive decoding and bounded below by the union of all fixed frequency-division regions, which are evaluated in Fig. 9 for Rayleigh fading.

The idea of reallocating bandwidth and power as the channel varies is closely related to dynamic channel allocation, where channel allocation is based on the noise (and interference) levels in a particular frequency band [5], [47]. The frequency allocation of (26) suggests that instead of using a threshold

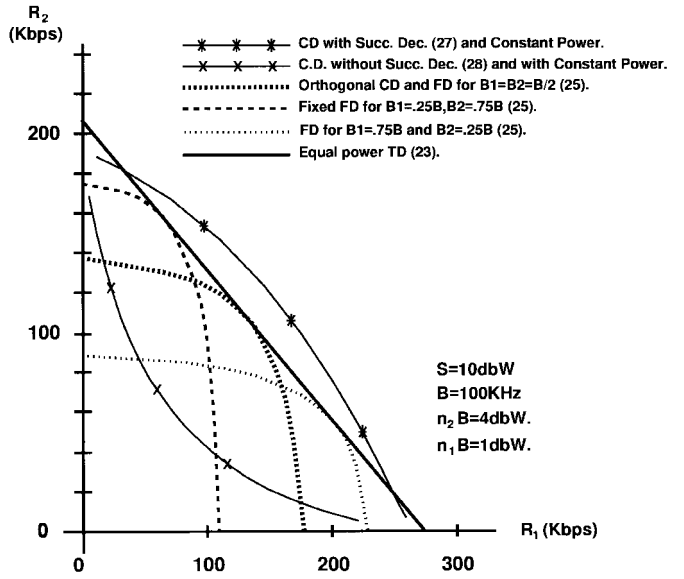

Fig. 9. Two-user capacity region in Rayleigh fading.

level to determine which user should occupy the channel, the channel should be allocated to the user which gets the most capacity from it. Similar ideas are currently being investigated for admission control [48].

D. Code-Division

We first consider superposition coding with successive decoding where, at each transmission, the multiresolution signal constellation is optimized relative to the instantaneous noise densities $n_1[i]$ and $n_2[i]$. In particular, the user with the lower noise density $n_j[i]$ at time i will subtract the interference caused by the other user, as was described in Section III-D. The rate region is thus the average of the rate regions in AWGN weighted by the joint probability of the noise densities

$$\left\{\bigcup\left(R_1 = B\int_k \log\left[1+\frac{S_{1,k}}{n_{1,k}B+S_{2,k}\mathbf{1}[n_{1,k}\geq n_{2,k}]}\right]\pi_k,\right.\right.$$
$$R_2 = B\int_k \log\left[1+\frac{S_{2,k}}{n_{2,k}B+S_{1,k}\mathbf{1}[n_{2,k}> n_{1,k}]}\right]\pi_k\Bigg);$$
$$\left.\int_k (S_{1,k}+S_{2,k})\pi_k = S\right\} \quad (27)$$

where $\mathbf{1}[\cdot]$ denotes the indicator function ($\mathbf{1}[x]=1$ if x is true and zero otherwise). Since superposition coding with successive decoding has a larger rate region than time- and frequency-division on the AWGN channel, we expect this to be true for the fading channel as well. Indeed, consider any rate point in the frequency-division capacity region (26). Associated with that point will be a set of frequency-divisions $(B_{1,k}, B_{2,k})$ and a set of transmit power values $(S_{1,k}, S_{2,k})$ corresponding to each noise pair $(n_{1,k}, n_{2,k})$. Let $S_k = S_{1,k}+S_{2,k}$. From Section III-D, for the broadcast channel with noise density values $(n_{1,k}, n_{2,k})$ there exists a superposition code with total power S_k that has a larger capacity region than frequency-division. Since we can find such a dominating code for all pairs of noise density values, the weighted integral of the superposition rates over all joint noise density pairs will exceed the frequency-division capacity region of (26).

The rate region for superposition coding without successive decoding is given by

$$\left\{\bigcup\left(R_1 = B\int_k \log\left[1+\frac{S_{1,k}}{n_{1,k}B+S_{2,k}}\right]\pi_k,\right.\right.$$
$$R_2 = B\int_k \log\left[1+\frac{S_{2,k}}{n_{2,k}B+S_{1,k}}\right]\pi_k\Bigg);$$
$$\left.\int_k (S_{1,k}+S_{2,k})\pi_k = S\right\}. \quad (28)$$

Since the capacity region corresponding to each k term in the integral (28) is bounded by a convex function, the resulting rate region will also be bounded by a convex function. Thus both the equal-power time-division rate region (23) and the frequency-division rate region (26), which are bounded by concave functions with the same endpoints, will have larger rate regions than that of (28).

Obtaining the code-division capacity region boundaries either with or without successive decoding requires either an exhaustive search or a two-dimensional optimization of the power over all time. However, we can lower-bound these regions by assuming a constant transmit power. This yields a point in the capacity region which is clearly beneath rate vectors obtained with optimal power adaptation. The resulting capacity region lower bound for Rayleigh fading is shown in Fig. 9, along with the time-division and fixed frequency-division rate regions, given by (23) and (25), respectively. The time-division and frequency-division regions are based on the maximum single-user capacity formula (5). From this figure we see that keeping the transmit power constant is clearly suboptimal, since the equal-power time-division rate region exceeds the region obtained by superposition code-division with successive decoding near the region end points. In light of this observation, it is interesting to recall our remark in Section II-B that keeping the transmit power constant has a negligible impact on the capacity of a single-user fading channel. We see now that the effect of power adaptation is much more pronounced in the multiuser case, where power adaptation impacts the interference on other users.

The capacity region for spread spectrum code-division with and without successive decoding are given by (27) and (28), respectively, with an addition bandwidth expansion term G. This term multiplies the numerator in the fractions of (27) and (28), and also divides the bandwidth term in front of their respective integrals. As in the AWGN case, this term will reduce the capacity region as G increases.

In Fig. 10 we compare the capacity regions in AWGN and in Rayleigh fading, assuming a constant transmit power. We show only the rate regions for code-division with and without successive decoding, since these regions bound the performance of time-division, frequency-division, and spread-spectrum coding with $G > 1$. We see that Rayleigh fading decreases the capacity region, as was also the case for the single-user channel.

To summarize the capacity results in this section, we calculate the time-varying capacity region by taking a weighted

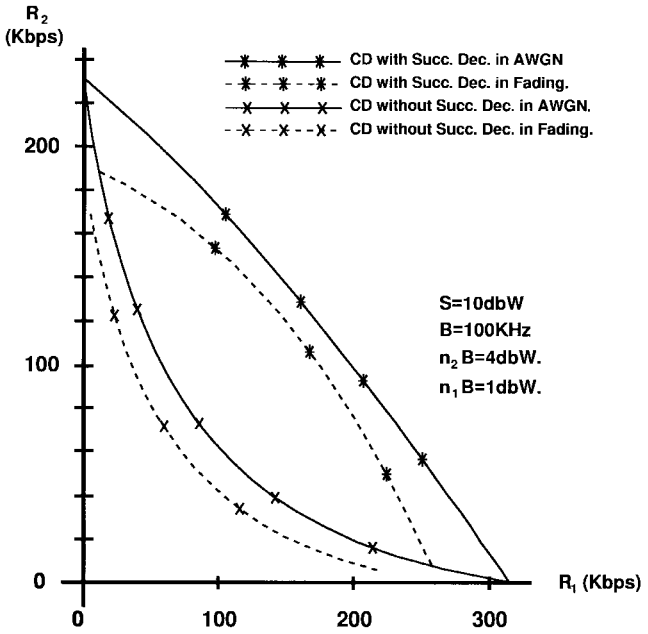

Fig. 10. Capacity region comparison in Rayleigh fading and in AWGN.

average of time-invariant capacity regions associated with the different noise density pairs, with the weights determined by the joint probability distribution of these pairs. Numerical evaluation of the capacity regions defined by (23) and (25) is straightforward using the methods defined in Section II-B. These regions have the same general shape as in Figs. 7 and 8, although they are smaller for the fading channel than for the AWGN channel. Evaluation of (26)–(28), requires an exhaustive search or a difficult multidimensional optimization over time. A lower bound for (26), the frequency-division rate region with optimal power and bandwidth adaptation, is obtained by maximizing over all fixed frequency-division rate regions (25). A lower bound for the code-division rate region with optimal power and transmit constellation adaptation is obtained by keeping the transmit power $S_{1,k} = S_{2,k} = S$ constant in (27) and (28).

V. Conclusions

We have compared the Shannon capacity region of the downlink fading channel under different spectrum-sharing techniques. We have shown that for both AWGN and fading channels, multiresolution coding with successive decoding and optimized code adaptation maximizes this capacity region. This optimal technique can be implemented using spread spectrum with successive interference cancellation, although the bandwidth expansion will result in some rate penalty. Frequency-division, time-division, and orthogonal code-division have equal rate regions if transmit power is varied according to the changing channel. In addition, dynamic channel (or timeslot) allocation will increase the efficiency of channel use. Finally, nonorthogonal coding without successive decoding or interference cancellation has the smallest capacity region.

Can we actually come close to these capacity limits? Clearly, the assumption of near-perfect channel estimates available at the transmitter and receiver is not feasible for rapidly varying channels. Issues of complexity and delay are swept under the rug for any capacity analysis, yet impose strong constraints in real system design. Finally, coordination of the dynamic resource allocation among multiple users in real time is also a challenge. However, adaptive rate and power transmission is currently receiving a great deal of attention, as is adaptive interference cancellation. As systems evolve to support different rate applications, the design philosophy that all users are created equal will vanish, and understanding achievable rate regions will become more important. Thus the purpose of this paper is not so much to suggest that we can achieve the capacity regions derived herein as it is to promote interest in the adaptive policies suggested by our analysis.

Acknowledgment

The author wishes to thank M. Honig for his insights about orthogonal spread-spectrum codes. The author would also like to thank the reviewers for their suggestions and insights.

References

[1] K. S. Gilhousen, I. M. Jacobs, R. Padovani, A. J. Viterbi, L. A. Weaver, Jr., and C. E. Wheatley III, "On the capacity of a cellular CDMA system," *IEEE Trans. Veh. Technol.*, vol. 40, pp. 303–312, May 1991.

[2] C.-L. I, L. J. Greenstein, and R. D. Gitlin, "A microcell/macrocell cellular architecture for low- and high-mobility wireless users," *IEEE J. Select. Areas Commun.*, vol. 11, pp. 885–891, Aug. 1993.

[3] P. Jung, P. W. Baier, and A. Steil, "Advantages of CDMA and spread spectrum techniques over FDMA and TDMA in cellular mobile radio applications," *IEEE Trans. Veh. Technol.*, vol. 42, pp. 357–364, Aug. 1993.

[4] B. Gundmundson, J. Sköld, and J. K. Ugland, "A comparison of CDMA and TDMA systems," in *IEEE Veh. Technol. Conf. Rec.*, May 1992, pp. 732–735.

[5] G. J. Pottie, "System design choices in personal communications," *IEEE Personal Commun. Mag.*, vol. 2, pp. 50–67, Oct. 1995.

[6] C. E. Shannon and W. Weaver, *A Mathematical Theory of Communication.* Urbana, IL: Univ. Illinois Press, 1949.

[7] A. D. Wyner, "Shannon theoretic approach to a Gaussian cellular multiple-access channel," *IEEE Trans. Inform. Theory*, vol. 40, pp. 1713–1727, Nov. 1994.

[8] T. S. Rappaport and L. B. Milstein, "Effects of radio propagation path loss on DS-CDMA cellular frequency reuse efficiency for the reverse channel," *IEEE Trans. Veh. Technol.*, vol. 41, pp. 231–242, Aug. 1992.

[9] J. G. Proakis, *Digital Communications*, 3rd ed. New York: McGraw-Hill, 1995.

[10] I. Kalet, "The multitone channel," *IEEE Trans. Commun.*, vol. 37, pp. 119–124, Feb. 1989.

[11] C. Berrou, A. Glavieux, and P. Thitimajshima, "Near Shannon limit error-correcting coding and decoding: Turbo codes," in *IEEE Int. Conf. Communications Rec.* (Geneva, Switzerland, May 1993), pp. 1064–1070.

[12] W. C. Y. Lee, "Estimate of channel capacity in Rayleigh fading environment," *IEEE Trans. Veh. Technol.*, vol. 39, pp. 187–189, Aug. 1990.

[13] J. M. Cioffi, G. P. Dudevoir, M. V. Eyuboglu, and G. D. Forney, "MMSE decision-feedback equalizers and coding, Part I: Equalization results and Part II: Coding results," *IEEE Trans. Commun.*, vol. 43, pp. 2595–2604, Oct. 1995.

[14] L. H. Ozarow, S. Shamai, and A. D. Wyner, "Information theoretic considerations for cellular mobile radio," *IEEE Trans. Veh. Technol.*, vol. 43, pp. 359–378, May 1994.

[15] T. Cover and J. Thomas, *Elements of Information Theory.* New York: Wiley, 1991.

[16] A. J. Viterbi, "Very low rate convolutional codes for maximum theoretical performance of spread-spectrum multiple-access channels," *IEEE J. Select. Areas Commun.*, vol. 8, pp. 641–649, May 1990.

[17] M. S. Alencar and I. F. Blake, "The capacity for a discrete-state code-division multiple-access channel," *IEEE J. Select. Areas Commun.*, vol. 12, pp. 925–937, June 1994.

[18] S. Verdú, "The capacity region of the symbol-asynchronous Gaussian multiple-access channel," *IEEE Trans. Inform. Theory*, vol. 35, pp. 735–751, July 1989.
[19] M. Rupf and J. L. Massey, "Optimum sequence multisets for symbol-synchronous code-division multiple-access channels," *IEEE Trans. Inform. Theory*, vol. 40, pp. 1261–1266, July 1994.
[20] A. A. Alsugair and R. S. Cheng, "Symmetric capacity and signal design for L-out-of-K symbol synchronous CDMA Gaussian channels," *IEEE Trans. Inform. Theory*, vol. 41, pp. 1072–1082, July 1995.
[21] A. M. Viterbi and A. J. Viterbi, "Erlang capacity of a power controlled CDMA system," *IEEE J. Select. Areas Commun.*, vol. 11, pp. 892–900, Aug. 1993.
[22] R. Prasad and A. Kegel, "Improved assessment of interference limits in cellular radio performance," *IEEE Trans. Veh. Technol.*, vol. 40, pp. 412–419, May 1991.
[23] R. G. Gallager, *Information Theory and Reliable Communication.* New York: Wiley, 1968.
[24] P. S. Chow, J. M. Cioffi, and J. A. C. Bingham, "A practical discrete multitone transceiver loading algorithm for data transmission over spectrally shaped channels," *IEEE Trans. Commun.*, vol. 43, Feb.–Apr. 1995.
[25] P. P. Bergmans and T. M. Cover, "Cooperative broadcasting," *IEEE Trans. Inform. Theory*, vol. IT-20, pp. 317–324, May 1974.
[26] S. Verdú, "Minimum probability of error for asynchronous Gaussian multiple-access channels," *IEEE Trans. Inform. Theory*, vol. IT-32, pp. 85–96, Jan. 1986.
[27] S. Yoshida and A. Ushirokawa "CDMA-AIC—Highly spectrum-efficient CDMA cellular-system based on adaptive interference cancellation," *IEICE Trans. Commun.*, vol. E79B, no. 3, pp. 353–360, Mar. 1996.
[28] P. Patel and J. Holtzman, "Analysis of a simple successive interference cancellation scheme in a DS-CDMA system," *IEEE J. Select. Areas Commun.*, vol. 12, pp. 796–807, June 1994.
[29] R. Lupas and S. Verdú, "Near–far resistance of multiuser detectors in asynchronous channel," *IEEE Trans. Commun.*, vol. 38, pp. 496–508, Apr. 1990.
[30] U. Madhow and M. L. Honig, "MMSE interference suppression for direct-sequence spread-spectrum CDMA," *IEEE Trans. Commun.*, vol. 42, pp. 3178–3188, Dec. 1994.
[31] Z. Xie, R. T. Short, and C. K. Rushforth, "A family of suboptimal detectors for coherent multiuser communications," *IEEE J. Select. Areas Commun.*, vol. 8, pp. 683–690, May 1990.
[32] A. Duel-Hallen, "A family of multiuser decision-feedback detectors for asynchronous code-division multiple access," *IEEE Trans. Commun.*, vol. 43, pp. 421–434, Feb./Mar./Apr. 1995.
[33] M. K. Varanasi and B. Aazhang, "Multistage detection in asynchronous code-division multiple-access communications," *IEEE Trans. Commun.*, vol. 38, pp. 509–519, Apr. 1990; see also "Near optimum detection in synchronous code-division multiple-access systems," *IEEE Trans. Commun.*, vol. 39, pp. 725–736, May 1991.
[34] Y. C. Yoon, R. Kohno, and H. Imai, "A spead-spectrum multiaccess system with cochannel interference cancellation," *IEEE J. Select. Areas Commun.*, vol. 11, pp. 1067–1075, Sept. 1993.
[35] A. Duel-Hallen, J. Holtzman, and Z. Zvonar, "Multiuser detection for CDMA systems," *IEEE Personal Commun. Mag.*, pp. 46–58, Apr. 1995.
[36] S. Shamai, L. H. Ozarow, and A. D. Wyner, "Information rates for a discrete-time Gaussian channel with intersymbol interference and stationary inputs," *IEEE Trans. Inform. Theory*, vol. 37, pp. 1527–1539, Nov. 1991.
[37] H. Schwarte, "Approaching the capacity of a continuous channel by discrete input distributions," *IEEE Trans. Inform. Theory*, vol. 42, pp. 671–675, Mar. 1996.
[38] I. Bar-David and S. Shamai, "On information transfer by envelope-constrained signals over the AWGN channel," *IEEE Trans. Inform. Theory*, vol. 34, pp. 371–379, May 1988.
[39] A. J. Viterbi and J. K. Omura, *Principles of Digital Communications and Coding.* New York: McGraw-Hill, 1979.
[40] A. J. Goldsmith and P. P. Varaiya, "Capacity of fading channels with channel side information," *IEEE Trans. Inform. Theory*, to be published. See also "Design and performance of high-speed communication systems in time-varying radio channels," Ph.D. dissertation, Dept. Elec. Eng. Comput. Sci., Univ. of Calif. at Berkeley, 1994. UCB/ERL Memo. M94/75.
[41] S.-G. Chua and A. J. Goldsmith, "Variable-rate variable-power MQAM for fading channels," in *IEEE Veh. Technol. Conf. Rec.* (Atlanta GA, Apr. 1996), pp. 815–819; also *IEEE Trans. Commun*, to be published.
[42] A. J. Goldsmith, "Variable-rate coded MQAM for fading channels," in *IEEE 1994 Globecom Communications Theory Miniconf. Rec.*, Nov. 1994, pp. 186–190.
[43] L.-F. Wei, "Coded modulation with unequal error protection," *IEEE Trans. Commun.*, vol. 41, pp. 1439–1449, Oct. 1993.
[44] P. P. Bergmans, "A simple converse for broadcast channels with additive white Gaussian noise," *IEEE Trans. Inform. Theory*, vol. IT-20, pp. 279–280, Mar. 1974.
[45] A. J. Viterbi, *CDMA: Principles of Spread Spectrum Communication.* Reading, MA: Addison Wesley, 1995.
[46] D. L. Schilling, L. B. Milstein, R. L. Pickholtz, M. Kullback, and F. Miller, "Spread spectrum for commercial communications," *IEEE Commun. Mag.*, pp. 66–79, Apr. 1991.
[47] J. C.-I. Chuang, "Performance issues and algorithms for dynamic channel assignment," *IEEE J. Sel. Areas Commun.*, vol. 11, pp. 955–963, Aug. 1993.
[48] N. Bambos and G. J. Pottie, "Power control based admission policies in cellular radio networks," in *IEEE GLOBECOM Conf. Rec.* (Orlando, FL, Dec. 1992), pp. 863–867.

Andrea J. Goldsmith (S'90–M'93) received the B.S. degree in electrical engineering and mathematics in 1986 and the M.S. and Ph.D. degrees in electrical engineering in 1991 and 1994, respectively, all from the University of California at Berkeley.

During her graduate studies, she was an IBM Fellow from 1993 to 1994. She is an Assistant Professor of electrical engineering at the California Institute of Technology, Pasadena. She was affiliated with Maximum Technologies from 1986 to 1990, and with AT&T Bell Laboratories from 1991 to 1992. Her research interests include wireless communications, Shannon theory, joint source/channel coding, and dynamic resource allocation in wireless networks.

Dr. Goldsmith was awarded the NSF Career Development Award in 1995, and the U.C. Berkeley David Griep Memorial Prize in 1991. She currently serves as technical editor for the IEEE TRANSACTIONS ON COMMUNICATIONS and the *IEEE Personal Communications Magazine*.